
Supporting Information

Amorphous gallium oxide homojunction-based optoelectronic synapse for multi-functional signal processing

Rongliang Li¹, Yonghui Lin¹, Yang Li^{1, 2, †}, Song Gao¹, Wenjing Yue¹, Hao Kan¹, Chunwei Zhang¹, and Guozhen Shen^{3, †}

¹School of Information Science and Engineering, University of Jinan, Jinan, 250022, China

²School of Microelectronics, Shandong University, Jinan 250101, China

³School of Integrated Circuits and Electronics, Beijing Institute of Technology, Beijing, 100081, China

Keywords: optoelectronic synapse; gallium oxide; filter; visual system; associative learning; logic gate

† Correspondence to: Y Li, yang.li@sdu.edu.cn; G Z Shen, gzshen@bit.edu.cn

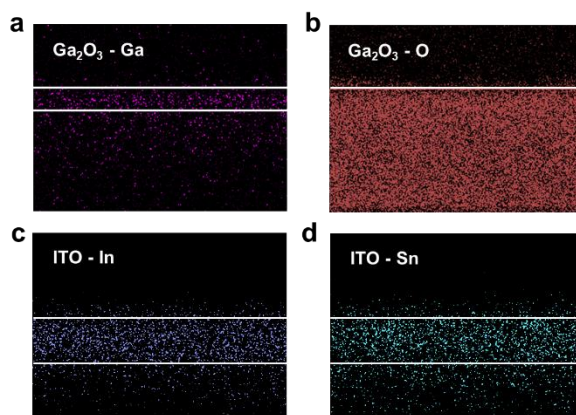


Fig. S1. The EDS spectra with Ga, O, In, and Sn elements of the device.

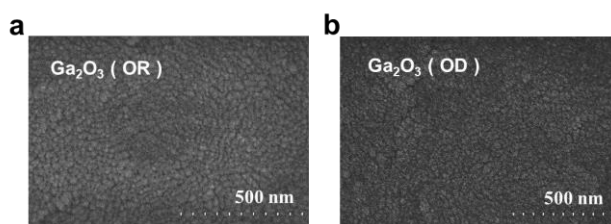


Fig. S2. The planar SEM of (a) Ga₂O₃(OR) and (b) Ga₂O₃(OD).

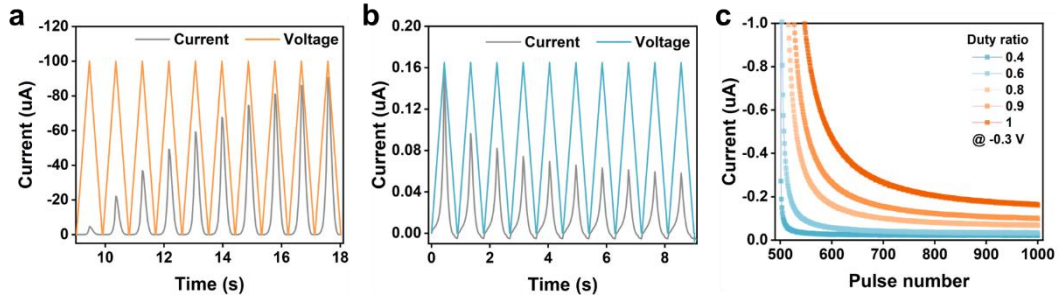


Fig. S3. The current sequence diagram by continuous 10 sequential sweeping curves at (a) negative voltage (0→-1 V→0) and (b) positive voltage (0→1 V→0). (c) The relaxation processes induced by varying LTP.

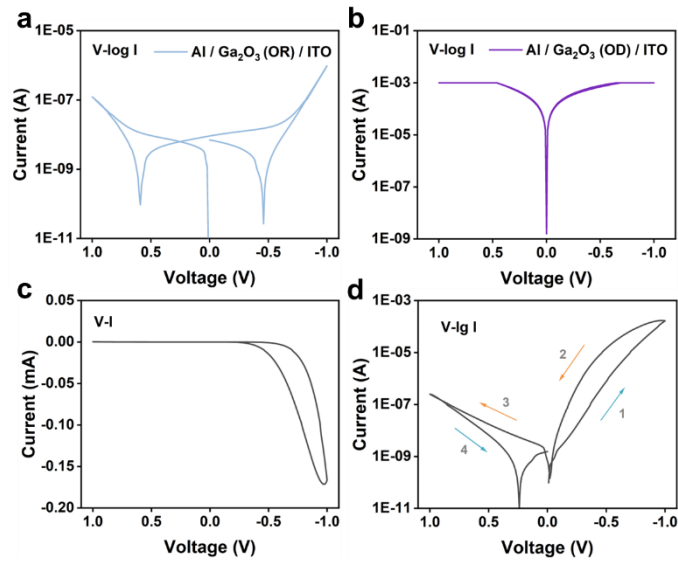


Fig. S4. The I-V curves of (a) Al/Ga₂O₃(OR)/ITO and (b) Al/Ga₂O₃(OD)/ITO. The (c) linear and (d) double-logarithmic I-V curve of Al/Ga₂O₃(OD)/Ga₂O₃(OR)/ITO.

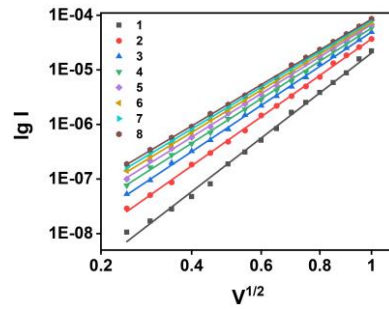


Fig. S5. The SE linear fitting curve of HRS under various cycles (1st-8th).

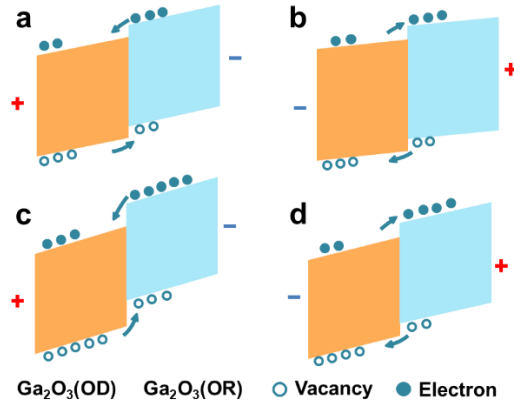


Fig. S6. Schematic diagram of carriers transferring in homojunction at (a, b) low voltage and (c, d) high voltage. There are potential barrier difference and oxygen concentration gradient between the $\text{Ga}_2\text{O}_3(\text{OD})$ and $\text{Ga}_2\text{O}_3(\text{OR})$. The electrons and vacancies will move along the barrier and oxygen concentration gradient under the positive voltage, leading to the reduction of potential barrier and the growth of current, while they move in the opposite direction under the negative voltage, resulting in the increase in potential barrier and the drop in current. And the varying applied voltage induces different changing of potential barrier and current.

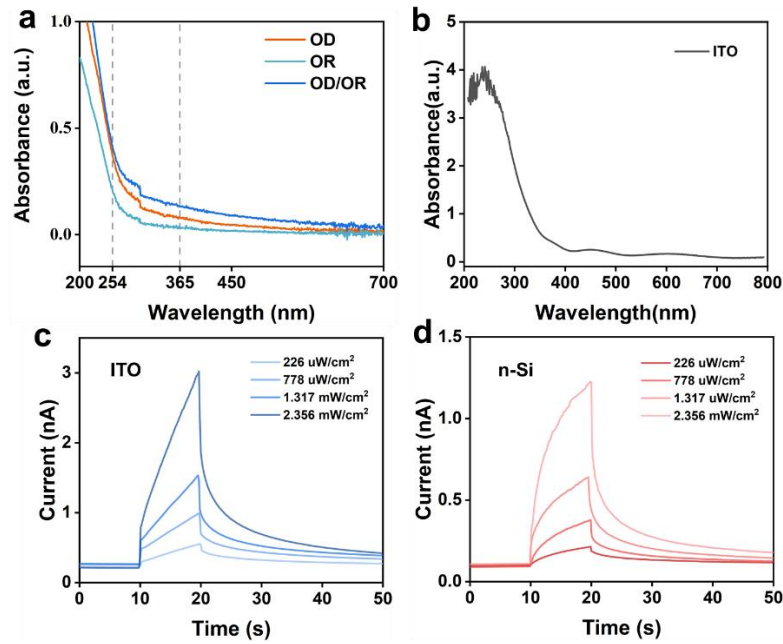


Fig. S7. The absorption spectrum of (a) $\text{Al}/\text{Ga}_2\text{O}_3(\text{OD})/\text{ITO}$, $\text{Al}/\text{Ga}_2\text{O}_3(\text{OR})/\text{ITO}$, $\text{Al}/\text{Ga}_2\text{O}_3(\text{OR})/\text{Ga}_2\text{O}_3(\text{OD})/\text{ITO}$ and (b) ITO . The comparison of synaptic behavior between (c) $\text{Al}/\text{Ga}_2\text{O}_3(\text{OR})/\text{Ga}_2\text{O}_3(\text{OD})/\text{ITO}$ and (d) $\text{n-Si}/\text{Ga}_2\text{O}_3(\text{OR})/\text{Ga}_2\text{O}_3(\text{OD})/\text{ITO}$.

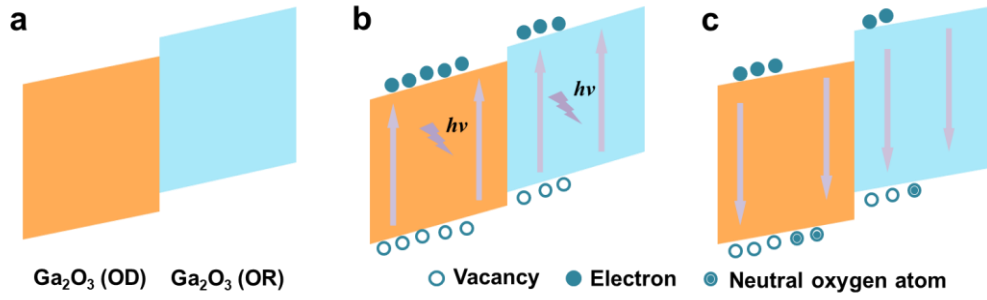


Fig. S8. The mechanism of optical synaptic behaviors under 254 nm light. (a) initial state without light. (b) Electron-hole pairs separation and potential barrier difference decrease under illumination. (c) Electron-hole pairs recombine or be trapped and potential barrier difference increases after the withdrawal of light.

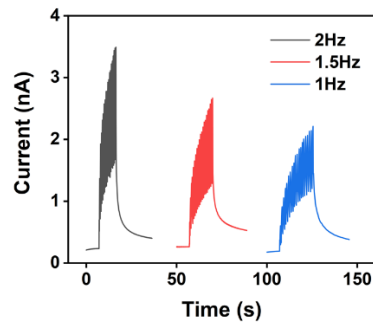


Fig. S9. The photocurrent responses triggered by 20 optical pulses with declining pulse frequencies (2 Hz, 1.5 Hz, and 1 Hz).

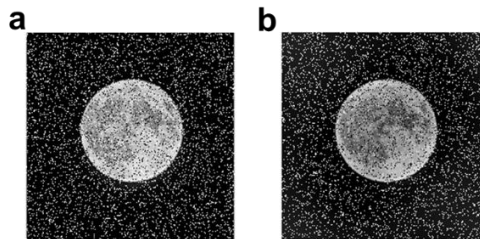


Fig. S10. The filtering process of the moon image with Salt-and-Pepper noise. (a) The original image with Salt-and-Pepper noise. (b) The high-pass filtered image.